

Time-resolved cathodoluminescence study of carrier relaxation in GaAs/AlGaAs layers grown on a patterned GaAs(001) substrate

D. H. Rich,^{a)} H. T. Lin, A. Konkar, P. Chen, and A. Madhukar
*Photonic Materials and Devices Laboratory, Department of Materials Science and Engineering,
 University of Southern California, Los Angeles, California 90089-0241*

(Received 4 March 1996; accepted for publication 22 May 1996)

We have examined the kinetics of carrier relaxation in three-dimensionally confined GaAs/AlGaAs layers obtained by growth on prepatterned GaAs(001) with time-resolved cathodoluminescence (CL). Time-delayed CL spectra at 87 K reveal that (i) relaxation of hot carriers into the largest 3D confined regions occurs on a time scale of a few hundred ps during the onset of luminescence, and (ii) the luminescence decay time also increases for these larger confined regions, owing to thermal reemission from QWs, diffusion across $\text{Al}_x\text{Ga}_{1-x}\text{As}$ barriers, and carrier feeding from surrounding thinner QWs. © 1996 American Institute of Physics. [S0003-6951(96)04331-8]

The growth of GaAs/ $\text{Al}_x\text{Ga}_{1-x}\text{As}$ nanostructures (quantum wires and boxes) on patterned GaAs substrates has attracted much attention in recent years.¹⁻⁵ The high quality of the heterolayers and interfaces that can be achieved during a single growth step circumvents the need for postgrowth etching and patterning on a nanoscale that can inevitably degrade the optical and structural quality of the nanostructure and its surrounding barriers. As a result of facet-dependent growth and cation migration rates, growth on prepatterned substrates can be used to attain a size reduction in the as-patterned micron-scale GaAs mesas so that the resulting size of three-dimensionally confined regions are on the order of ~ 100 Å.¹⁻³ From a fundamental perspective, the study of quantum boxes fabricated on isolated mesas should permit a simple understanding of the temperature and excitation dependence of its optical properties. Such isolated nanostructures on regular arrays inherently avoid a more complex environment of thermally excited electrons and holes that can potentially interact with several quantum boxes, as in the cases for the self-organized InAs island growth.^{6,7} A basic issue which needs to be addressed with the growth of nanostructures on mesas concerns the tailoring of the structure in a manner that maximizes carrier capture and collection into the quantum box. Studies of carrier thermalization and collection have been performed for GaAs/ $\text{Al}_x\text{Ga}_{1-x}\text{As}$ quantum wires grown into V-shaped grooves.⁸ From a device viewpoint, the efficiency of carrier collection in the nanostructure determines the quantum efficiency of the quantum wire or box laser.

In this letter, we examine the kinetics of carrier relaxation and spatial distribution of luminescence in 3D confined GaAs/ $\text{Al}_x\text{Ga}_{1-x}\text{As}$ regions using time-resolved cathodoluminescence (CL). We show that thermalization of carriers in GaAs/ $\text{Al}_x\text{Ga}_{1-x}\text{As}$ layers comprising the mesa sidewalls influence both the carrier capture time and luminescence decay time in the 3D confined GaAs volumes situated under the mesa pinch-off region. These results are expected to influence current thinking in the design and growth of 3D confined GaAs volumes so that a maximum collection efficiency of carriers in the quantum box can be achieved.

The details of the sample preparation and procedure for

size-reducing molecular beam epitaxial growth have been previously reported for growth on GaAs(111)B and GaAs(001) substrates.¹⁻³ For this study, GaAs(001) substrates were patterned along $\langle 100 \rangle$ directions using conventional photolithography followed by wet chemical etching to give square mesas with $\sim 3-4$ μm long edges and $\sim 2-3$ μm in vertical height. The growth consisted of a size-reducing buffer consisting of four periods of 175 ML $\text{Al}_{0.25}\text{Ga}_{0.75}\text{As}/25$ GaAs followed by a 40 period multiple quantum well (MQW) composed of 40 ML $\text{Al}_{0.25}\text{Ga}_{0.75}\text{As}/20$ ML GaAs (1 ML = 2.83 Å). A detailed study of this growth procedure, utilizing transmission electron microscopy (TEM), showed that the evolution of the growth on the mesa sidewalls involves the formation of $\{103\}$ and $\{101\}$ facets bounding the (001) surface layers on the mesa top.³ A cross-sectional TEM of a typical mesa after growth is shown in Fig. 1(a). A pinch-off region is identified by the arrow in Fig. 1(a), which shows the final full (001) GaAs layer prior to mesa shrinkage to an apex. The lateral confinement in the final stage of pinch-off due to the negligible growth on the $\{101\}$ sidewalls is also observed. The

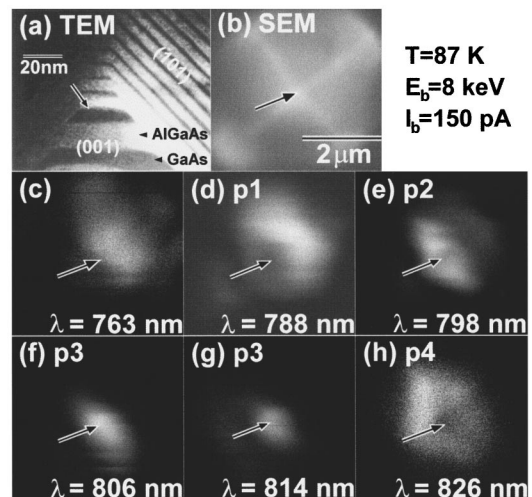


FIG. 1. (a) TEM, (b) SEM, and monochromatic CL images at various wavelengths (c)–(h) of a typical mesa. The arrows in (b)–(h) point to the mesa top where pinchoff occurred. The length scale for images (c)–(h) is indicated in the SEM image. CL imaging parameters are indicated in the upper-right-hand side of the figure.

^{a)}Electronic mail: danrich@alnitak.usc.edu

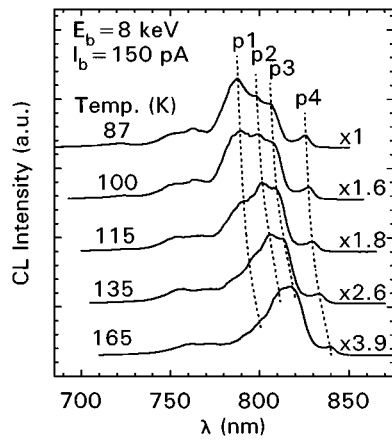


FIG. 2. Constant excitation CL spectra taken with various samples temperatures in the $87 \leq T \leq 165$ K range. The wavelength shift in peaks, $p1-p4$, with temperature is illustrated with the dashed lines.

arrow indicates a GaAs volume whose lateral dimensions are 440, 275, and 100 Å for the bottom, top, and height of the trapezoid, respectively, thereby clearly delineating a GaAs region expected to exhibit quantum confinement effects. Owing to the interfacet cation migration and facet-dependent growth rates, an increase in the QW and barrier thickness of the (001) layers relative to the as-deposited MQW is observed in Fig. 1(a). Subsequent growth after pinch-off results in a ~ 0.2 - μm -thick short period GaAs/AlGaAs MQW on the sidewalls whose well width, w , varies mainly from ~ 10 – 50 Å.

The CL experiments were performed with a modified JEOL-840A scanning electron microscope (SEM) using an 8 keV electron beam with probe current of 150 pA, corresponding to a low excitation condition.⁹ The temperature of the sample was varied from 87 to 200 K in this study. Monochromatic CL images of the mesas were obtained at 87 K. Time-resolved CL experiments were performed with the method of delayed coincidence in an inverted single photon counting mode, with a time resolution of ~ 100 ps.¹⁰ Electron beam pulses of 50 ns width with a 1 MHz repetition rate were used to excite the sample. The luminescence signal was dispersed by a 1/4 monochromator and detected by a cooled GaAs:Cs PMT. Time-delayed CL spectra were acquired with a spectral resolution of ~ 1 nm.

Results of constant excitation CL imaging and spectroscopy are shown in Figs. 1 and 2, respectively. A SEM image of a different but again typical mesa is shown in Fig. 1(b). The arrows in Figs. 1(b)–1(h) point to the mesa top. The CL images of this mesa are shown for increasing wavelengths in the 763–826 nm range in Figs. 1(c)–1(h). The CL spectra were taken with the beam rastered about a $\sim 1 \mu\text{m} \times 1 \mu\text{m}$ region centered at the mesa top, thereby giving a spatial average over this region. Various sample temperatures were examined, as shown in Fig. 2. Three identifiable peaks, labeled $p1-p3$, are observed to lie within the intense broad luminescence feature located in the $780 \leq \lambda \leq 815$ nm range. A fourth peak, $p4$, has its peak emission at 826 nm for $T = 87$ K, and is identified as emission from the underlying 525 ML GaAs layers. Peaks $p1-p3$ are observed to follow the shift of the GaAs peak with temperature, and originate

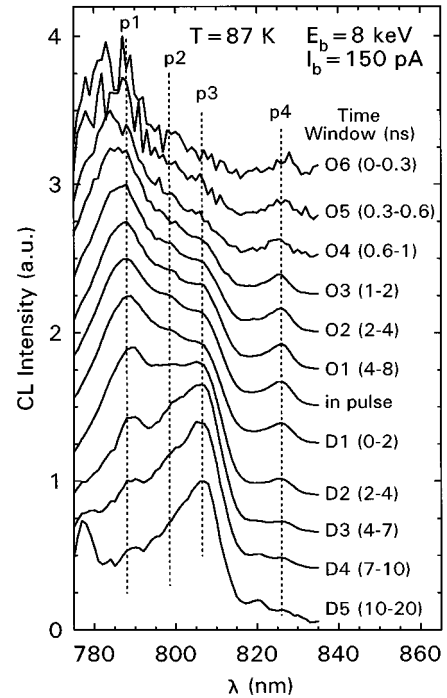


FIG. 3. Time delayed CL spectra shown with various onset (O_i) and decay (D_i) time windows. All spectra are renormalized to have about the same maximum peak height. Peak positions $p1-p4$, corresponding to values determined from the constant excitation CL spectra, are indicated by the vertical dashed lines.

from the various GaAs/Al_xGa_{1-x}As layers grown on the mesa. As observed in the CL imaging, emissions at different wavelengths have varying degrees of localization about the mesa top. Images in Figs. 1(c) and 1(d) show that the luminescence at 763 and 788 nm, respectively, is primarily from regions along the sidewalls away from the mesa top. As the wavelength increases from 798 to 814 nm [Figs. 1(e)–1(g)] we observe a greater localization of luminescence about the mesa top. Calculations of the $n=1$ electron to heavy-hole ($e1-hh1$) transition energy in Al_{0.25}Ga_{0.75}As/GaAs QWs at $T=87$ K show that the $780 \leq \lambda \leq 815$ nm range corresponds to QW widths in the $48 \leq w \leq 130$ Å range. Additional smaller peaks are observed in the $723 \leq \lambda \leq 760$ nm range, corresponding to $16 \leq w \leq 32$ Å. Thus, in connecting the CL observations with the above TEM measurements, we conclude that emission involving $\lambda \leq 800$ nm ($w \leq 75$ Å) is attributed to luminescence from the sidewall QWs, while emission in the $805 \leq \lambda \leq 815$ nm range originates from the thick ($90 \leq w \leq 130$ Å) QWs below the pinch-off region.

The temperature dependence of the CL spectra shown in Fig. 2 reveals salient aspects concerning the thermalization of carriers. For temperatures increasing from 87 to 165 K, the peak intensity of $p1$ decreases rapidly relative to that for $p3$. This is consistent with a larger thermal reemission of carriers from thinner QWs relative to thicker QWs for this temperature range. Despite the larger carrier capture rate in short period MQWs due to quantum capture,¹¹ the larger $e1-hh1$ energies in thinner QWs likewise reduce the barrier height for thermal reemission,^{12,13} leading to a marked reduction in QW luminescence efficiency at these higher temperatures. The relative increase in $p3$ therefore suggests that

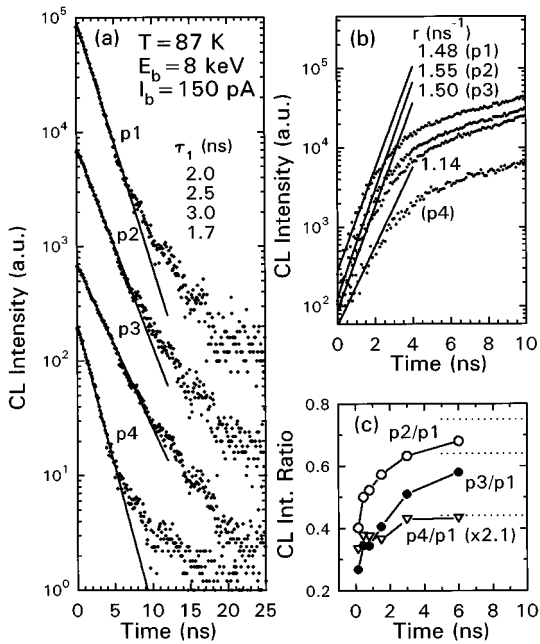


FIG. 4. CL transients for peaks $p1-p4$. The decay curves in (a) show linear fits for the initial ~ 6 ns of decay. The resulting initial luminescence decay times, τ_1 , are indicated. The onset curves are shown in (b), with a linear fit for the first ~ 2 ns. The rates, r , of increase are indicated for $p1-p4$. CL peak intensity ratios for $p2/p1$, $p3/p1$, and $p4/p1$ are shown in (c) for various onset times from 150 ps to 6 ns.

these hot carriers are able to diffuse over sub- μm distances, further facilitating collection in the 3D confined regions beneath the pinch-off layer.

In order to further examine these thermalization effects, we have measured time-delayed CL spectra at $T=87$ K for the various time windows indicated in Fig. 3. The time windows $O6-O1$ and $D1-D5$ denote time windows relative to the beginning of *onset* and *decay*, respectively, of the luminescence, as referred to the beginning and end of the electron beam pulses. The CL intensity of peaks $p1-p4$ is shown versus time for both the decay and onset stages in Figs. 4(a) and 4(b), respectively. It is evident that rapid capture occurs for the carriers giving rise to the $p1$ feature, as this is the strongest emission for the $O6$ window centered at 150 ps. The other features, $p2-p4$, rapidly grow in the 0–2 ns range; the peak intensity ratios, $p2/p1$, $p3/p1$, and $p4/p1$, versus onset time are shown in Fig. 4(c). Peak $p1$ is also visibly blue shifted ~ 10 nm during the $O6$ and $O5$ windows (centered at 150 and 450 ps) and gradually toward the 788 nm position observed in spectra measured during constant excitation (Fig. 2) and in the center of the 50 ns excitation pulse (labeled *in pulse* in Fig. 3). Again, the narrower QWs and barriers comprising $p1$ are expected to exhibit the faster quantum capture times. Subsequent re-emission of these carriers on a time scale of a few hundred ps and thermalization into the thicker QWs comprising $p1$ give rise to the gradual red shift observed for windows $O6-O1$. Likewise, these

carriers are also able to thermalize and diffuse over distances of $\sim 0.1-0.5 \mu\text{m}$ to the thicker QWs giving rise to peaks $p2$, $p3$, and $p4$. These large distances are reflected in the relatively slow onset rates shown in Fig. 4(b). We define an onset rate, r , as $r = \Delta \ln(I_{pi}) / \Delta t$, and is given by slopes of the tangents to the onset curves of Fig. 4(b). A reduced rate of 1.14 ns^{-1} for $p4$ compared to that for $p1-p3$ reflects the larger distances from the sidewalls ($\sim 0.5 \mu\text{m}$) that hot carriers must traverse before recombining in the thick 525 ML GaAs layers.

During the decay stage of the luminescence, further red shifts of peaks $p1$ and $p3$ are detected in the $D1-D5$ windows. An initial luminescence decay time, τ_1 , is measured from the slopes in the $\ln(I_{pi})$ versus time transients. As shown in Fig. 4(a), τ_1 increases in the sequence 2.0, 2.5, and 3.0 ns, respectively, for peaks $p1$, $p2$, and $p3$. Again, we expect the enhanced thermal re-emission of carriers in the thinner QW sidewalls ($p1$ and $p2$) to continuously feed the larger GaAs volumes represented by the $p3$ feature, as the system proceeds towards equilibrium.

In conclusion, these results illustrate convincingly that the collection of carriers into the larger QWs and 3D confined GaAs volumes occurs as a result of thermalization, reemission, and diffusive transport of carriers from the thinner QWs comprising the sidewalls. The thinner sidewall QWs in this study have conveniently served as *optical markers*, in addition to their intended purpose of structural markers, thereby providing key signatures in the wavelength and time domain that allow for a visualization of the carrier relaxation. It is anticipated, therefore, that a suitable choice of cladding layers during future designs of size-reducing growth will enhance the efficiency of carrier collection into quantum boxes residing just below the pinch-off region.

This work was supported by ARO, AFOSR, and NSF (RIA-ECS).

- ¹A. Madhukar, K. C. Rajkumar, and P. Chen, Appl. Phys. Lett. **62**, 1547 (1993), and references therein.
- ²K. C. Rajkumar, A. Madhukar, K. Rammohan, D. H. Rich, P. Chen, and L. Chen, Appl. Phys. Lett. **63**, 2905 (1993).
- ³A. Konkar, K. C. Rajkumar, Q. Xie, P. Chen, A. Madhukar, H. T. Lin, and D. H. Rich, J. Cryst. Growth **150**, 311 (1995).
- ⁴E. Kapon, M. C. Tamargo, and D. M. Hwang, Appl. Phys. Lett. **50**, 347 (1987).
- ⁵E. Kapon, D. M. Hwang, and R. Bhat, Phys. Rev. Lett. **63**, 430 (1989).
- ⁶D. Leonard, M. Krishnamurthy, C. M. Reaves, S. P. Denbaars, and P. M. Petroff, Appl. Phys. Lett. **63**, 3203 (1993).
- ⁷M. Grundmann *et al.*, Phys. Rev. Lett. **74**, 4043 (1995).
- ⁸J. Christen, M. Grundmann, E. Kapon, E. Colas, D. M. Hwang, and D. Bimberg, Appl. Phys. Lett. **61**, 67 (1992).
- ⁹D. H. Rich *et al.*, Phys. Rev. B **43**, 6836 (1991).
- ¹⁰D. Bimberg, H. Münzel, A. Steckenborn, and J. Christen, Phys. Rev. B **31**, 7788 (1985).
- ¹¹B. Deveaud, J. Shah, T. C. Damen, and W. T. Tsang, Appl. Phys. Lett. **52**, 1886 (1988).
- ¹²U. Jahn, J. Menniger, R. Hey, and H. T. Grahn, Appl. Phys. Lett. **64**, 2382 (1994).
- ¹³K. Rammohan, H. T. Lin, D. H. Rich, and A. Larsson, J. Appl. Phys. **78**, 6687 (1995).